

Joint User Scheduling and Resource Allocation for Millimeter Wave Systems Relying on Adaptive-Resolution ADCs

Xihan Chen, *Student Member, IEEE*, Yunlong Cai, *Senior Member, IEEE*,
An Liu, *Senior Member, IEEE*, and Lajos Hanzo, *Fellow, IEEE*,

Abstract—Millimeter wave (mmWave) communication systems using adaptive-resolution analog-to-digital converters (RADCs) have recently drawn considerable interests from the research community as benefit of their high energy efficiency and low implementation cost. In this paper, we focus on the mmWave uplink using RADCs and investigate the joint user scheduling and resource allocation problem. Specifically, we seek to maximize the system throughput of the scheduled users by jointly optimizing their transmit power level and hybrid combiners as well as the number of quantization bits, subject to practical constraints. By relying on fractional programming (FP) techniques, we first covert this problem into a form amenable to optimization and exploit the specific structures in its solutions with the aid of the so-called Ky Fan n -norm. Then, the resultant optimization problem is solved using a penalty block successive concave approximation (P-BSCA) algorithm. Our numerical results reveal that the proposed algorithm substantially enhances the throughput of the scheduled users compared to the state-of-the-art benchmark schemes and provides more flexible and efficient resource allocation control.

I. INTRODUCTION

To meet the ever-increasing data rate requirements, the amalgamation of millimeter wave (mmWave) and massive multiple-input multiple-output (MIMO) techniques is becoming an evident trend for future wireless networks. However, the implementation of these techniques may not be practical, because their fully digital implementation requires a dedicated radio frequency (RF) chain relying on power-thirsty high-resolution analog-to-digital converters (ADCs) for each antenna element. Hence, utilizing hybrid combiners using low-resolution ADCs (LADCs) could be a natural technique of addressing these power consumption concerns. Therefore substantial research efforts have been invested in their channel estimation and beamforming design [1]–[3].

However, the performance of mmWave systems with LADCs is limited by the coarse quantization, especially in the low signal-to-noise ratio (SNR) regime. To circumvent this difficulty, the authors of [4] first proposed a more energy-efficient mmWave receiver architecture using adaptive-resolution ADCs (AR-ADCs) for massive MIMO schemes. Moreover, a pair of ingenious quantization bit allocation strategies were developed for minimizing the quantization error effects subject to a constraint on the total ADC power. On the other hand, user scheduling is another critical problem for mmWave systems employing AR-ADCs, which significantly affects the interference pattern in the uplink. Therefore, it is desirable to take them into account when conceiving the resource allocation strategies for data transmission, especially when the number of potential users is huge but the available network resources

are limited. Although the authors of [5] have developed a user scheduling algorithm for mmWave systems using LADCs, there is a paucity of literature on the joint user scheduling and resource allocation problem using AR-ADCs. This is because the allocation of quantization bits at each AR-ADC would exacerbate the final decision of user scheduling, thereby substantially affecting the communications between the base station (BS) and the users.

Motivated by these observations, we focus our attention on the uplink of mmWave systems using AR-ADCs and investigate the joint user scheduling and resource allocation problem. Specifically, we seek to maximize the system throughput of the scheduled users by jointly optimizing the transmit power level and hybrid combiners and allocating the quantization bits, subject to the user scheduling constraint, transmit power constraint, the constraints related to the quantization bits, as well as the unit modulus constraint on the elements of the analog combining matrix.

It is quite a challenge to globally solve the problem formulated, which has a complex objective function (OF) relying on multiple ratio terms and a combinatorial constraint. By leveraging sophisticated fractional programming techniques [8], we first recast the original problem into an equivalent form more amenable to optimization. To overcome the difficulty arising from the combinatorial constraint, we devise a novel sparsity-enhancing technique for its solutions with the aid of Ky Fan n -norm [10]. The benefit of this is that the choice of the smoothing parameters in the conventional l_p -norm based heuristic algorithms is no longer critical [9]. Then we propose an efficient *penalty block successive approximation* (P-BSCA) algorithm for the resultant problem. Our numerical results reveal that the proposed algorithm achieves a remarkable performance gain over the relevant benchmark schemes.

II. SYSTEM MODEL AND PROBLEM FORMULATION

Let us now consider the uplink of a multiuser mmWave system, where K single-antenna users are distributed within a specific geographical area and the BS is equipped with a uniform linear array (ULA) of M antennas and $S \ll M$ RF chains. Specifically, the BS schedules $N \leq S$ users for transmission in each time slot, and the set of scheduled users is denoted by \mathcal{N} . For convenience, we focus our attention on the block-fading channels model, i.e. all channels remain time-invariant in each fading block. Then the signal received at the BS can be expressed as

$$\mathbf{y} = \sum_{k=1}^K \sqrt{p_k} \mathbf{h}_k x_k + \mathbf{w} = \mathbf{H} \mathbf{P}^{\frac{1}{2}} \mathbf{x} + \mathbf{w}, \quad (1)$$

where $\mathbf{H} \triangleq [\mathbf{h}_1, \dots, \mathbf{h}_K]$ with $\mathbf{h}_k \in \mathbb{C}^M \times 1$ is the uplink channel vector from user k to the BS, $\mathbf{P} \triangleq \text{diag}(p_1, \dots, p_K)$ with p_k is the transmit power level of user k , $\mathbf{x} \triangleq$

X. Chen, Y. Cai and A. Liu are with the College of Information Science and Electronic Engineering, Zhejiang University, Hangzhou 310027, China (e-mail: chenxihan, ylcai, anliu@zju.edu.cn).

L. Hanzo is with the Department of Electronics and Computer Science, University of Southampton, Southampton SO17 1BJ, U.K. (e-mail: lh@ecs.soton.ac.uk).

$[x_1, \dots, x_K]^T$ with $x_k \sim \mathcal{CN}(0, 1)$ specifying the data symbol of user k , and $\mathbf{w} \in \mathbb{C}^{M \times 1}$ is an additive white Gaussian noise (AWGN) vector with zero mean and unit variance.

The BS implements a hybrid combiner to reap the full benefits of massive MIMO and for mitigating the effects of quantization errors imposed by the AR-ADC, which results in a reduced hardware cost and power consumption. Let $\Phi \in \mathbb{C}^{M \times S}$ denote the BS's analog combiner, which is usually implemented using phase shifters and its entries obey the unit modulus constraint, i.e. we have $|\Phi(m, s)| = 1, \forall m, s$. Then, the signal combined by the analog combiner can be represented by $\bar{\mathbf{y}} = \Phi^H \mathbf{y}$. For tractability, the linear additive quantization noise model (AQNM) is introduced for characterizing the quantization process [6], where the imaginary or real component of the s -th element in $\bar{\mathbf{y}}$ is quantized by each AR-ADC using d_s quantization bits. In this case, the quantized signal can be expressed as

$$\mathbf{y}_q = \mathcal{D}(\bar{\mathbf{y}}) = \mathbf{D}_\rho \bar{\mathbf{y}} + \mathbf{w}_q, \quad (2)$$

where $\mathcal{D}(\cdot)$ refers to the element-wise quantization operation, $\mathbf{D}_\rho \triangleq \text{diag}(\rho_1, \dots, \rho_S)$ with $\rho_s = 1 - \zeta_s$ is the diagonal matrix of quantization gains, and $\zeta_s \triangleq \frac{\pi\sqrt{3}}{2} 4^{-d_s}$ stands for the normalized quantization error; \mathbf{w}_q is the additive quantization noise independent of $\bar{\mathbf{y}}$, which obeys the complex Gaussian distribution with zero mean and covariance matrix $\mathbf{C}_q = \mathbf{D}_\rho \mathbf{D}_\zeta \text{diag}(\Phi^H \mathbf{H} \mathbf{P} \mathbf{H} \Phi + \Phi^H \Phi)$, where $\mathbf{D}_\zeta \triangleq \text{diag}(\zeta_1, \dots, \zeta_S)$. Note that in contrast to the conventional fixed-resolution ADCs, AR-ADCs can adapt the number of quantization bits to the propagation characteristics, thereby providing additional flexibility for these mmWave systems.

Then, the quantized signal \mathbf{y}_q is successively processed by the BS's digital combiner $\mathbf{F} \in \mathbb{C}^{S \times S}$ and the linear receiver beamformer $\mathbf{v}_k \in \mathbb{C}^S$ so as to mitigate the multiuser interference and alleviate the quantization loss, which yields the recovered signal of user k in the form of:

$$\hat{x}_k = \mathbf{v}_k^H \mathbf{F}^H \mathbf{D}_\rho \Phi^H \mathbf{H} \mathbf{P}^{\frac{1}{2}} \mathbf{x}_k + \mathbf{v}_k^H \mathbf{F}^H \mathbf{D}_\rho \Phi^H \mathbf{w} + \mathbf{v}_k^H \mathbf{F}^H \mathbf{w}_q.$$

For ease of exposition, we let ϕ denote the phase vector of the BS's vectorized analog combiner $\text{vec}(\Phi)$, $\mathbf{p} \triangleq [p_1, \dots, p_K]^T$, $\mathbf{d} \triangleq [d_1, \dots, d_S]^T$, $\mathbf{v} \triangleq [v_1^T, \dots, v_K^T]^T$, $\mathbf{f} = \text{vec}(\mathbf{F})$, and $\xi \triangleq [\mathbf{p}^T, \phi^T, \mathbf{d}^T, \mathbf{v}^T, \mathbf{f}^T]^T$. As such, the achievable throughput of user k can be expressed as $r_k(\xi) = \log_2(1 + \eta_k(\xi))$, where $\eta_k(\xi)$ stands for the signal-to-interference-noise ratio (SINR) of user k defined in (3) at the bottom of this page.

The key observation is that the uplink interference pattern heavily relies on the choice of which specific users to schedule in this time slot. To this end, we seek to maximize the system throughput among the scheduled users by jointly optimizing

the uplink scheduling, hybrid combiner design, and quantization bits allocation under practical constraints. Instead of directly determining the discrete scheduling variables, we treat the uplink users in an implicit manner with the aid of power control, depending on whether the transmit power level of user k is positive. This optimization problem is formulated as:

$$\mathcal{P} : \max_{\xi} \sum_{k=1}^K r_k(\xi) \quad (4a)$$

$$\text{s.t. } \|\mathbf{p}\|_0 = N, \quad (4b)$$

$$0 \leq p_k \leq P_k^{\max}, \forall k, \quad (4c)$$

$$d_s^{\min} \leq d_s \leq d_s^{\max} \text{ is an integer, } \forall s, \quad (4d)$$

$$\sum_{s=1}^S d_s \leq S d_{\text{avg}}, \quad (4e)$$

$$\phi \in \Upsilon \triangleq [0, 2\pi]^{MS}, \quad (4f)$$

where $\|\cdot\|_0$ refers to the l_0 -norm operator, P_k^{\max} specifies the maximum transmit power of user k , d_s^{\min} and d_s^{\max} respectively denote the minimum and maximum number of quantization bits in the RF chain s , and d_{avg} is the average number of quantization bits across the different RF chains. The constraint (4b) ensures that the number of users scheduled in each time slot is equivalent to N , while the constraint (4e) represents the quantization bits budget at the BS. Finally, the constraint (4f) corresponds to the unit modulus constraint on the elements of the analog combining matrix.

III. PENALTY BLOCK SUCCESSIVE CONCAVE APPROXIMATION ALGORITHM

Problem \mathcal{P} is challenging to handle because 1) the optimization variables ξ are intricately coupled in the non-concave OF of (4a); 2) the discrete variables involved in the quantization bits allocation and the presence of l_0 -norm in (4b) make the feasible set non-concave, which further complicates its solution. In this section, we propose a novel P-BSCA algorithm which efficiently combines the penalty method with the block successive concave approximation (BSCA) method [7] to find the stationary solution of problem \mathcal{P} .

A. Problem Reformulation

To facilitate an efficient algorithmic design, we first exploit the complex quadratic and Lagrangian dual transform [8] for recasting problem \mathcal{P} into a series of simple equivalent problems:

$$\mathcal{P}_1 : \max_{\xi, \eta, \nu} \sum_{k=1}^K f_k(\xi, \eta, \nu) \quad \text{s.t.} \quad (4b) - (4f),$$

$$\eta_k(\xi) = \frac{p_k |\mathbf{v}_k^H \mathbf{F}^H \mathbf{D}_\rho \Phi^H \mathbf{h}_k|^2}{\sum_{l \neq k} p_l |\mathbf{v}_k^H \mathbf{F}^H \mathbf{D}_\rho \Phi^H \mathbf{h}_l|^2 + |\mathbf{v}_k^H \mathbf{F}^H \mathbf{D}_\rho \Phi^H|^2 + \mathbf{v}_k^H \mathbf{F}^H \mathbf{C}_q \mathbf{F} \mathbf{v}_k}. \quad (3)$$

$$f_k(\xi, \eta, \nu) = 2\Re\{\sqrt{p_k(1 + \eta_k)} \nu_k^H \mathbf{v}_k^H \mathbf{F}^H \mathbf{D}_\rho \Phi^H \mathbf{h}_k\} + \log_2(1 + \eta_k) - \eta_k - \nu_k^H \nu_k \omega_k(\xi), \quad (5)$$

$$\omega_k(\xi) = \sum_{l=1}^K p_l |\mathbf{v}_k^H \mathbf{F}^H \mathbf{D}_\rho \Phi^H \mathbf{h}_l|^2 + |\mathbf{v}_k^H \mathbf{F}^H \mathbf{D}_\rho \Phi^H|^2 + \mathbf{v}_k^H \mathbf{F}^H \mathbf{C}_q \mathbf{F} \mathbf{v}_k. \quad (6)$$

where the objective function $f_k(\boldsymbol{\xi}, \boldsymbol{\eta}, \boldsymbol{\nu})$ associated with $\omega_k(\boldsymbol{\xi})$ is defined in (5)-(6) at the bottom of the next page, $\boldsymbol{\eta} = [\eta_1, \dots, \eta_K]^T$ stands for the auxiliary variable introduced for the SINR within the rate expression, and $\boldsymbol{\nu} = [\nu_1, \dots, \nu_K]^T$ represents the auxiliary variables introduced to achieve the desired decoupling between the numerator and denominator in the SINR.

To make the problem tractable, we relax the discrete constraint on the number of quantization bits d_s into a continuous one, yielding

$$d_s^{\min} \leq d_s \leq d_s^{\max}, \quad (7)$$

and then round the solution d_s^* of the relaxed problem to its nearest integer [11] as follows

$$\bar{d}_s(\varepsilon) = \begin{cases} \lfloor d_s^* \rfloor, & \text{if } d_s^* - \lfloor d_s^* \rfloor \leq \varepsilon \quad \forall s, \\ \lceil d_s^* \rceil, & \text{otherwise,} \end{cases} \quad (8)$$

where the hyper-parameter $\varepsilon \in [0, 1]$ is efficiently searched via the bisection method, so that we have $\sum_{s=1}^S \bar{d}_s(\varepsilon) \leq S d_{\text{avg}}$.

It is worth noting that solving problem \mathcal{P}_1 is still difficult due to the non-concave l_0 -norm constraint (4b). A promising solution is to leverage the smoothed l_p -norm [9] followed by the iteratively reweighted l_2 -norm minimization algorithm to construct a tight surrogate function for the l_0 -norm, thereby inducing the sparsity structure in uplink power control. However, the convergence properties of the l_p -norm based algorithms are crucially dependent on the specific choice of the smoothing parameters, which may not be suitable for practical implementations due to the associated dynamic system requirements. To this end, we devise a novel technique of enhancing the sparsity structures in the solutions for problem \mathcal{P}_1 with the aid of the Ky Fan n -norm of [10], [12]. Specifically, we represent the l_0 -norm in form of the difference between the l_1 -norm and Ky Fan n -norm as follows:

$$\|\mathbf{p}\|_0 = \min\{n : \|\mathbf{p}\|_1 - \|\mathbf{p}\|_n = 0, \forall 0 \leq n \leq N\}, \quad (9)$$

where $\|\mathbf{p}\|_1 \triangleq \sum_{k=1}^K |p_k|$ stands for the l_1 -norm, and $\|\mathbf{p}\|_n$ represents the Ky Fan n -norm given by the sum of largest n absolute values, i.e.,

$$\|\mathbf{p}\|_n = \sum_{i=1}^n |p_{\chi(i)}|, \quad (10)$$

where χ specifies the permutation of $\{1, \dots, K\}$ in descending order such that we have $|p_{\chi(1)}| \geq \dots \geq |p_{\chi(K)}|$. Using the above notations, the constraint (4b) reduces to $\|\mathbf{p}\|_1 - \|\mathbf{p}\|_N = 0$.

Now, we are ready to apply the penalty method to solve problem \mathcal{P}_1 . For the problem at hand, the first step is to incorporate the penalty term associated with the equality constraint $\|\mathbf{p}\|_1 = \|\mathbf{p}\|_N$ and to obtain the penalized version of \mathcal{P}_1 as

$$\mathcal{P}_2 : \max_{\boldsymbol{\xi}, \boldsymbol{\eta}, \boldsymbol{\nu}} \sum_{k=1}^K f_k(\boldsymbol{\xi}, \boldsymbol{\eta}, \boldsymbol{\nu}) - \lambda(\|\mathbf{p}\|_1 - \|\mathbf{p}\|_N) \quad (11a)$$

$$\text{s.t.} \quad (4c) - (4f), \quad (11b)$$

where λ is a positive penalty parameter that characterizes the cost of violating the equality constraint.

Algorithm 1 Proposed P-BSCA Algorithm for Problem (4)

Initialization: Initialize the algorithm with a feasible point $\boldsymbol{\xi}^0$. Set the accuracy tolerance β , the maximum inner iteration number I , the maximum outer iteration number T , $t = 0$, $i = 0$, $\alpha > 1$, and $\lambda^0 > 0$.

Repeat

Repeat

- Update $\boldsymbol{\eta}^{i+1}$, $\boldsymbol{\nu}^{i+1}$, and \mathbf{f}^{i+1} by applying its first-order optimality condition in sequence.
- Construct a surrogate function $\hat{g}^i(\mathbf{d})$ and update \mathbf{d}^{i+1} by solving problem (13).
- Construct a surrogate function $\hat{g}^i(\boldsymbol{\phi})$ and update $\boldsymbol{\phi}^{i+1}$ according to (14).
- Update \mathbf{p}^{i+1} by solving problem (20).

Until the value of (11a) converges or reaching the maximum inner iteration number I . Otherwise, let $i \leftarrow i + 1$.

Update the penalty parameter: $\lambda^{t+1} = \alpha \lambda^t$.

Until the value of the penalty term is less than β or $t \geq T$. Otherwise, let $t \leftarrow t + 1$.

B. The Algorithm Proposed for Solving Problem \mathcal{P}_2

In this subsection, we present the proposed P-BSCA algorithm for solving problem \mathcal{P}_2 , mainly consisting of twin loops. Specifically, we increase the value of the penalty parameter λ to reduce the equality constraint violation at each outer iteration, while the BSCA method is utilized for updating the optimization variables in different blocks within the inner iteration. Note that the constraints in problem \mathcal{P}_2 are separable, consequently we can partition the design variables into six independent blocks. Hereinafter, we introduce the superscripts i and t for representing the variables associated with the i -th inner and the t -th outer iteration, respectively. Then we elaborate on the implementation details of the proposed P-BSCA algorithm at the i -th inner iteration within the t -th outer iteration.

1) **Optimization of $\boldsymbol{\eta}$:** When fixing the other variables, the optimal $\boldsymbol{\eta}^*$ can be uniquely determined by examining the first-order optimality condition, which is defined in (3).

2) **Optimization of $\boldsymbol{\nu}$:** The subproblem w.r.t. $\boldsymbol{\nu}$ can be further decoupled on a per-user basis, and each one is an unconstrained quadratic optimization problem, which can be efficiently solved by setting $\partial f_k / \partial \nu_k = 0$, that is

$$\nu_k^* = \omega_k^{-1}(\boldsymbol{\xi}) \sqrt{p_k(1 + \eta_k)} \mathbf{v}_k^H \mathbf{F}^H \mathbf{D}_\rho \boldsymbol{\Phi}^H \mathbf{h}_k. \quad (12)$$

3) **Optimization of \mathbf{f} :** Similar to the subproblem w.r.t. $\boldsymbol{\nu}$, the subproblem w.r.t. \mathbf{f} is also unconstrained as well as quadratic, and can be solved by checking its first-order optimality condition. The details are omitted due to the limited space.

4) **Optimization of \mathbf{d} :** Now we turn attention to the subproblem w.r.t. \mathbf{d} , which features a non-concave OF subject to the linearly coupled constraint (4e). To handle this complex problem, we resort to the SCA method for approximating the OF as a sequence of concave surrogate functions, which is given by

$$\hat{g}^i(\mathbf{d}) = \sum_{k=1}^K (f_k(\mathbf{d}^i) + \nabla_{\mathbf{d}}^T f_k(\mathbf{d}^i)(\mathbf{d} - \mathbf{d}^i)) - \tau_d \|\mathbf{d} - \mathbf{d}^i\|^2,$$

where $\nabla_d f_k(\mathbf{d}^i)$ is the partial derivative of $f_k(\mathbf{d})$ w.r.t. \mathbf{d} at the current point \mathbf{d}^i , and τ_d is a positive constant. Note that the term $\tau_d \|\mathbf{d} - \mathbf{d}^i\|^2$ is added to ensure that $\hat{g}_k^i(\mathbf{d})$ is a lower bound of the original objective function, which plays a crucial role in guaranteeing the algorithm's convergence. Thus, finding the optimal \mathbf{d}^* amounts to solving the following linearly constrained quadratic problem:

$$\max_{\mathbf{d}} \hat{g}^i(\mathbf{d}) \quad \text{s.t. (4e) and (7),} \quad (13)$$

which can be efficiently solved by the generic interior-point method using off-the-shelf solvers, such as CVX.

5) **Optimization of ϕ** : Let us now consider the subproblem w.r.t. ϕ , which can be formulated as $\max_{\phi \in \Upsilon} \sum_{k=1}^K f_k(\phi)$. Following the same approach as used for updating \mathbf{d} , a concave surrogate function $\hat{g}^i(\phi)$ is judiciously constructed to circumvent the difficulty arising from the non-concave nature of the OF, which can be expressed as

$$\hat{g}^i(\phi) = \sum_{k=1}^K (f_k(\phi^i) + \nabla_{\phi}^T f_k(\phi^i)(\phi - \phi^i)) - \tau_{\phi} \|\phi - \phi^i\|^2,$$

where τ_{ϕ} is a positive constant and $\nabla_{\phi} f_k(\phi^i)$ is the partial derivative of $f_k(\phi)$ w.r.t. ϕ at the current point ϕ^i .

Consequently, the optimal solution ϕ^* of the approximated problem $\max_{\phi \in \Upsilon} \hat{g}^i(\phi)$ is equivalent to the projection of the gradient $\phi^i + \nabla_{\phi}^T f_k(\phi^i)/\tau_{\phi}$ onto the box feasible region Υ , which yields a closed-form solution as

$$\phi^* = \mathbb{P}_{\Upsilon}[\phi^i + \nabla_{\phi}^T f_k(\phi^i)/\tau_{\phi}], \quad (14)$$

where $\mathbb{P}_{\Upsilon}[\cdot]$ refers to the projection over the feasible set Υ .

6) **Optimization of \mathbf{p}** : To fully exploit the intrinsic structure of the subproblem w.r.t. \mathbf{p} , we first rewrite its non-concave OF into a difference-of-concave (DC) form, i.e.,

$$\sum_{k=1}^K f_k(\mathbf{p}) - \lambda(\|\mathbf{p}\|_1 - \|\mathbf{p}\|_N) = g(\mathbf{p}) - h(\mathbf{p}), \quad (15)$$

where $g(\mathbf{p})$ and $h(\mathbf{p})$ respectively are strongly concave functions given by

$$g(\mathbf{p}) = \sum_{k=1}^K f_k(\mathbf{p}) - \lambda\|\mathbf{p}\|_1 - \tau_p \|\mathbf{p}\|^2, \quad (16)$$

$$h(\mathbf{p}) = -\lambda\|\mathbf{p}\|_N - \tau_p \|\mathbf{p}\|^2. \quad (17)$$

By linearizing the strongly concave function $h(\mathbf{p})$ based on the first-order Taylor expansion and the current point \mathbf{p}^i , we can obtain

$$\hat{h}^i(\mathbf{p}) = h(\mathbf{p}^i) + \partial_{\mathbf{p}}^T h(\mathbf{p}^i)(\mathbf{p} - \mathbf{p}^i), \quad (18)$$

where $\partial_{\mathbf{p}} h(\mathbf{p}^i)$ stands for the subgradient of $h(\mathbf{p})$ w.r.t. \mathbf{p} at the current point \mathbf{p}^i . Specifically, the subgradient of $h(\mathbf{p})$ w.r.t. \mathbf{p} can be analytically computed as

$$\partial_{\mathbf{p}} h(\mathbf{p}) = -\tau_p \mathbf{p} - \lambda \partial \|\mathbf{p}\|_N, \quad (19)$$

where $\partial \|\mathbf{p}\|_N$ is the subgradient of $\|\mathbf{p}\|_N$ calculated as

$$j\text{-th entry of } \partial \|\mathbf{p}\|_N = \begin{cases} \text{sgn}(p_j), & \text{if } |p_j| \geq |p_{\chi(N)}| \\ 0, & \text{otherwise.} \end{cases}$$

Hence, in the i -th iteration of the proposed P-BSCA algorithm, we have the following approximated convex problem:

$$\max_{\mathbf{p}} g(\mathbf{p}) - \hat{h}^i(\mathbf{p}) \quad \text{s.t. (4c),} \quad (20)$$

which can be uniquely determined by standard convex optimization methods.

C. Complete Algorithm

According to the above derivations, we summarize the proposed P-BSCA procedure in Algorithm 1. Here, we remark that by appropriately tuning the penalty parameter in each outer iteration, the limiting point ξ^* generated by the proposed P-BSCA algorithm would essentially meet the equality constraint (4b). As such, we can show that the proposed P-BSCA algorithm converges to a stationary solution of problem \mathcal{P} . The proof is similar to that of [13], and we hence omit the details for simplicity. Let us now further analyze the computational complexity. In each iteration of the proposed P-BSCA algorithm, we solve the subproblems for the six blocks of variables sequentially. Then, the overall computational complexity of the proposed algorithm is dominated by updating $\{\mathbf{f}, \phi\}$ and is given by $O(T_1 I_1 (S^6 + S^2 M + K M^2))$, where I_1 and T_1 respectively denote the maximum inner and outer iteration numbers.

IV. NUMERICAL RESULTS

This section presents our numerical results for quantifying the performance of the proposed algorithm, whilst providing essential insights. For all simulations, unless otherwise specified, we consider a single-cell network configuration of radius $r = 500$ m, where a total of $K = 40$ candidate users are randomly distributed and the BS is equipped with $M = 96$ antennas and $S = 32$ RF chains to schedule $N = 16$ users for their uplink transmission. We adopt the extended Saleh-Valenzuela geometric model for our mmWave channels [14], where the large-scale path loss of the user k -BS link is given by $\gamma_k[\text{dB}] = 72 + 29.2 \log_{10} \mu_k + \psi$, μ_k stands for the corresponding distance, and $\psi \sim \mathcal{CN}(0, 1)$ is the log-normal shadowing. The channel bandwidth is 10 MHz, and the background noise is -174 dBm/Hz. Furthermore, we set $P_k^{\max} = 10$ dBm, $d_s^{\max} = 8$, $d_s^{\min} = 1$, and $d_{\text{avg}} = 3$ [15]. For the proposed P-BSCA algorithm, we choose $\lambda^0 = 10^{-3}$ and $\alpha = 1.8$. Three schemes are included as benchmarks: 1) the smooth l_p/l_2 approximation (SA) scheme of [12], which adopts the quadratic form of the weighted mixed l_p/l_2 -norm for inducing the sparsity in user scheduling and jointly optimizes the other variables by maximizing the system throughput. 2) the uniform allocation (UA) scheme of [5], where the LADCs with uniform quantization bits are implemented and all variables are jointly optimized for maximizing the system's throughput. 3) random scheduling (RS) scheme, where the scheduled users are randomly selected and the other variables are optimized for maximizing the system throughput.

We commence by examining the convergence behavior of the proposed P-BSCA algorithm. Fig. 1 (a) and (b) respectively plot an instance of the average sum rate and the value of penalty versus the number of iterations. It is observed that the proposed P-BSCA promptly converges to a stationary solution within a few iterations, while the penalty value reduces below a threshold of 10^{-3} at the same time. These results demonstrate the ability of the proposed P-BSCA algorithm to efficiently handle the combinatorial constraint (4b) of problem \mathcal{P} .

Fig. 2 (a) depicts the average sum rate versus the maximum transmit power P^{\max} for different schemes. We notice that the average sum rate achieved by all schemes is monotonically

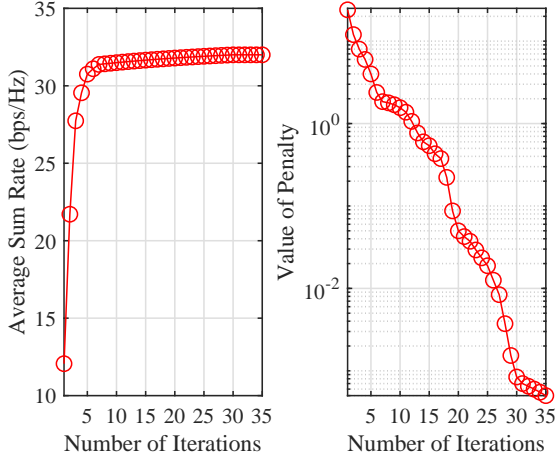


Fig. 1: Convergence performance of the proposed P-BSCA algorithm: (a) average sum rate; (b) the value of penalty.

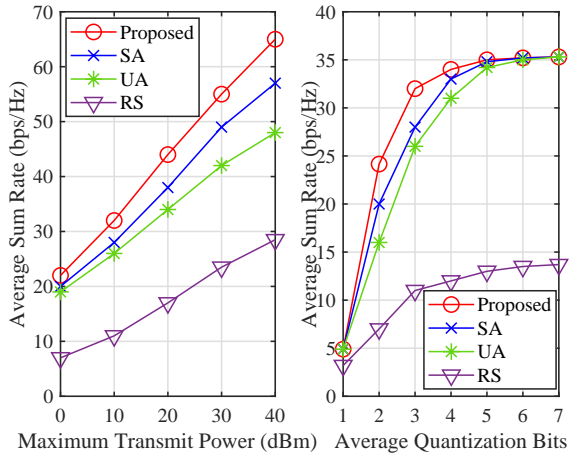


Fig. 2: Average sum rate versus (a) maximum transmit power P^{\max} and (b) the number of average quantization bits d_{avg} .

increasing with the maximum transmit power. Furthermore, it is observed that the proposed P-BSCA scheme can outperform all the other competing schemes, and its improvement becomes more significant as the maximum transmit power increases. The reason for this trend is that the proposed P-BSCA scheme can exploit the distinctive channel characteristics of different candidate users to facilitate more efficient user scheduling and resource allocation strategies, which also demonstrates the importance of our joint optimization based design. In a nutshell, it appears that for mmWave systems having ample transmit power, our proposed P-BSCA scheme is particularly attractive from an optimum resource allocation perspective.

In Fig. 2 (b), we plot the average sum rate versus the number of average quantization bits d_{avg} for different schemes. It is interesting to note that the average sum rates of the proposed P-BSCA, SA, and UA schemes nearly coincide both at low and high average number of quantization bits. This is due to the following reasons: 1) For a low average number of quantization bits there is no additional freedom for adapting the allocation of quantization bits depending on the specific

propagation conditions of the different users. 2) When the number of average quantization bits is sufficiently high, the quantization errors due to ADCs can be neglected and thus it is no longer the primary bottleneck of mmWave systems. Additionally, we observe that the proposed P-BSCA scheme generally attains a higher average sum rate than the SA/UA scheme for a moderate average number of quantization bits, thanks to our novel sparsity enhancement approach based on the Ky Fan n -norm and to the more flexible quantization bit allocation. On the other hand, it can be seen that the performance of the RS scheme is much worse than that of all the other competing schemes, due to the lack of a more efficient user scheduling strategy.

V. CONCLUSION

In this contribution, we have investigated the joint user scheduling and resource allocation problem of mmWave systems using AR-ADCs. Specifically, we maximized the system throughput of the scheduled users by jointly optimizing the transmit power level and hybrid combiners as well as allocating the quantization bits under some practical constraints. optimized to maximize the sum throughput of the scheduled users under some practical constraints. To solve such a non-convex combinational problem efficiently, we conceived a novel P-BSCA iterative algorithm. Finally, our numerical results demonstrate the efficiency of the proposed algorithm.

REFERENCES

- [1] J. Choi et al., "Near maximum-likelihood detector and channel estimator for uplink multiuser massive MIMO systems with one-bit ADCs," *IEEE Trans. Commun.*, vol. 64, no.5, pp. 2005-2018, Mar. 2016.
- [2] J. Mo et al., "Hybrid architectures with few-bit ADC receivers: Achievable rates and energy-rate tradeoffs," *IEEE Trans. Wireless Commun.*, vol. 16, no. 4, pp. 2274-2287, Apr. 2017.
- [3] H. Sheng et al., "Energy efficiency optimization for beamspace massive MIMO systems with low-resolution ADCs," in *Proc. IEEE Wireless Commun. Netw. Conf. (WCNC)*, Seoul, Korea, May 2020, pp. 1-7.
- [4] J. Choi et al., "Resolution-adaptive hybrid MIMO architectures for millimeter wave communications," *IEEE Trans. Signal Process.*, vol. 65, no. 23, pp. 6201-6216, Dec. 2017.
- [5] J. Choi et al., "User scheduling for millimeter wave hybrid beamforming systems with low-resolution ADCs," *IEEE Trans. Wireless Commun.*, vol. 18, no. 4, pp. 2401-2414, Apr. 2019.
- [6] O. Orhan et al., "Low power analog-to-digital conversion in millimeter wave systems: Impact of resolution and bandwidth on performance," *Proc. Inf. Theory Appl. Workshop (ITA)*, pp. 191-198, Feb. 2015.
- [7] M. Razaviyan, "Successive convex approximation: Analysis and applications," Ph.D. dissertation, Univ. Minnesota, Minneapolis, MN, USA, 2014.
- [8] K. Shen and W. Yu, "Fractional programming for communication systems-Part II: Uplink scheduling via matching," *IEEE Trans. Signal Process.*, vol. 66, no. 10, pp. 2631-2644, May 2018.
- [9] Y. Shi et al., "Smoothed-minimization for green cloud-RAN with user admission control," *IEEE J. Sel. Areas. Commun.*, vol. 34, no. 4, pp. 1022-1036, Apr. 2016.
- [10] K. Fan, "Maximum properties and inequalities for the eigenvalues of completely continuous operators," *Proc. Nat. Academy Sci.*, vol. 37, no. 11, pp. 760-766, 1951.
- [11] A. Liu et al., "Two-timescale hybrid compression and forward for massive MIMO aided C-RAN," *IEEE Trans. Signal Process.*, vol. 67, no. 9, pp. 2484-2498, May 2019.
- [12] K. Yang et al., "Federated learning via over-the-air computation," *IEEE Trans. Wireless Commun.*, vol. 19, no. 3, pp. 2022-2035, Mar. 2020.
- [13] Y. Cai et al., "Joint transceiver design for secure downlink communications over an amplify-and-forward MIMO relay," *IEEE Trans. Commun.*, vol. 65, no. 9, pp. 3691-3704, Sep. 2017.
- [14] Adel A. M. Saleh and Reinaldo A. Valenzuela, "A statistical model for indoor multipath propagation," *IEEE J. Sel. Areas Commun.*, vol. 5, no. 2, pp. 128-137, Feb. 1987.
- [15] H. Sheng et al., "Energy efficiency optimization for millimeter wave system with resolution-adaptive ADCs," *IEEE Wireless Lett.*, DOI: 10.1109/LWC.2020.2995908.